Received: 18 April 2020 | Accepted: 12 August 2020

DOI: 10.1111/gcb.15322

PRIMARY RESEARCH ARTICLE

Global Change Biology WILEY

Accelerated rate of vegetation green-up related to warming at northern high latitudes

Hoonyoung Park[1,2] | Sujong Jeong[1,2] | Josep Peñuelas[3,4]

[1]Department of Environmental Planning, Graduate School of Environmental Studies, Seoul National University, Seoul, Republic of Korea

[2]Institute for Sustainable Development (ISD), Seoul National University, Seoul, Republic of Korea

[3]CSIC, Global Ecology Unit CREAF-CSIC-UAB, Bellaterra, Spain

[4]CREAF, Cerdanyola del Vallès, Bellaterra, Spain

Correspondence
Sujong Jeong, Department of Environmental Planning, Graduate School of Environmental Studies, Seoul National University, Seoul, Republic of Korea.
Email: sujong@snu.ac.kr

Funding information
National Research Foundation of Korea: , Grant/Award Number: 2019R1C1C1004826 and 2019R1A2C3002868; Creative-Pioneering Researchers Program of Seoul National University; European Research Council Synergy, Grant/Award Number: ERC-2013-SyG-610028 IMBALANCE-P

Abstract

Mid- to high-latitude vegetation are experiencing changes in their seasonal cycles as a result of climate change. Although the rates of seasonal growth from winter dormancy to summer maturity have accelerated because of changes in environmental conditions, less attention has been paid to the rate of vegetation green-up (RVG) and its dynamics, which could advance vegetation maturity. We analyzed the long-term changes in RVG and the drivers at high northern latitudes for 35 years (1982–2016) using satellite-retrieved leaf area index data based on partial correlation analyses and multivariable linear regression. The rates tended to increase significantly with time, particularly at high latitudes above 60°N in North America (1.8% mon^{-1} $decade^{-1}$, $p < .01$) and Eurasia (1.0% mon^{-1} $decade^{-1}$, $p < .01$). The increasing trend in North America was mostly because of increased heat accumulation in spring (1.2% mon^{-1} $decade^{-1}$), that is, more rapid green-up owing to warming, with an increased carbon dioxide concentration (0.6 mon^{-1} $decade^{-1}$). The trend in Eurasia, however, was induced by warming, increased carbon dioxide concentration, and stronger radiation, 1.0%, 0.7%, and 0.5% mon^{-1} $decade^{-1}$, respectively, but was partly counteracted by earlier pregreen-up dates of −1.2% mon^{-1} $decade^{-1}$, that is, earlier initiation of growth which counteracted green-up rate acceleration. The results suggested that warming was the predominant factor influencing the accelerated RVG at high latitudes; however, Eurasian vegetation exhibited different green-up dynamics, mitigating the influence of warming with the earlier pregreen-up. Our findings imply that high-latitude warming will drive vegetation seasonality toward rapid green-up and early maturity, leading to the reinforcement of climate–vegetation interactions; however, the consequences will be more distinct in North America owing to the absence of alleviation by earlier pregreen-up.

KEYWORDS
green-up dynamics, high-latitude vegetation, leaf area index, rate of vegetation green-up, spring warming, vegetation phenology

1 | INTRODUCTION

Vegetation shifts their seasonal growth cycles as an adaptation to changes in climatic and environmental conditions in a warming world (Peñuelas & Filella, 2001; Piao et al., 2020; Schwartz, 2013). Earlier growing seasons is one of the most distinct vegetation seasonality responses (Richardson et al., 2013). Surface observations focusing on local areas (Baldocchi, 2020; Menzel et al., 2006; Richardson

et al., 2010) and spaceborne remote sensing of the continents (Badeck et al., 2004; Jeong et al., 2011; Park et al., 2018) have revealed that the beginning of growing seasons has advanced over the last few decades in the northern extratropics. In addition to earlier springs, vegetation maturity, that is, the peak of growing seasons, has advanced at northern mid- and high latitudes when compared to earlier decades (Gonsamo et al., 2018; Xu et al., 2016). Such shifts from the start to the peak are clear signs of the effects of climate change on terrestrial ecosystems (Buitenwerf et al., 2015). However, our knowledge of vegetation seasonality is largely biased toward discrete events and their shifts rather than continuous development in the green-up or decay in the senescence stage (Clark et al., 2014; Kern et al., 2020; Park et al., 2015; Seyednasrollah et al., 2018). Therefore, more focus is needed on understanding the changes in development in the green-up to better predict vegetation dynamics related to climate change.

Observations from traditional ground and satellite phenologies (e.g., budburst, foliar unfolding, and the start of growing season) are effective tools for diagnosing the seasonality of terrestrial ecosystems (Jeong et al., 2011; Piao et al., 2020; Richardson et al., 2010). Especially, satellite data provides large-scale and long-term observations with a regular time interval, which is necessary to monitor the continuous green-up of vegetation. The rate of vegetation green-up (RVG), which refers to the rate of canopy development from winter dormancy to summer maturity, is one of the continuous aspects of seasonality (Klosterman, Hufkens, & Richardson, 2018; Park et al., 2015; Pettorelli et al., 2005; Reed et al., 1994; Seyednasrollah et al., 2018). Park et al. (2015) showed that the RVG has nonlinear relationships with spring temperature in deciduous forests. Seyednasrollah et al. (2018) demonstrated the relationships of RVG to temperature and moisture deficit in several ecosystems in the southeastern part of North America. Kern et al. (2020) highlighted that the green-up duration, inversely proportional to the RVG, is affected by the growth onset as well as meteorological variables in Central Europe. These studies suggest that the RVG is a dynamic factor which responds to the changes in environmental conditions and transforms the entire shape of the green-up stage together with the growth onset (Kern et al., 2020; Klosterman et al., 2018; Park et al., 2015). Wang et al. (2018) presented that the RVG accelerated over the past several decades from a global perspective. They pointed out that global warming could be the reason of the acceleration based on correlations of the RVG with temperature and precipitation. Their indication raises the necessity for clarifying the acceleration in RVG and its mechanisms especially at high latitudes considering the increasing level of climate change in future (Stocker et al., 2013).

This study investigated RVG and its trends over a 35 year period based on satellite-retrieved leaf area index (LAI) data in the northern extratropics from 1982 to 2016. First, we investigated the distribution and interannual patterns between RVG and the peak of the growing season to elucidate the influence of RVG on seasonal growth. We also conducted partial correlation analyses of RVG to investigate the complex responses of growth rate to environmental variables. In addition, we investigated the long-term RVG trends and its key drivers based on a multilinear approach to identify the mechanisms of RVG acceleration. This study aimed to deepen our understanding on the seasonal growth of vegetation by highlighting its continuous aspect together with vegetation phenologies. The results of the present study could reveal insights into the growth dynamics in the green-up stage.

2 | MATERIALS AND METHODS

2.1 | Data

2.1.1 | Satellite-retrieved LAI and land-cover classification

We used the third generation of the Global Inventory Modeling and Mapping Studies Leaf Area Index (GIMMS LAI3g) v4 (Zhu et al., 2013) to examine RVG in the northern extratropics. GIMMS LAI3g covered the globe from 1982 to 2016 at a high spatiotemporal resolution—a 1/12° latitude–longitude grid and a 15 day time interval. As the largest dataset of satellite-retrieved LAI, GIMMS LAI3g has been invaluable in many previous studies in the identification of various changes in terrestrial ecosystems (Park et al., 2018; Piao et al., 2020; Zhu et al., 2016).

We used the UMd (University of Maryland, Department of Geography) global land-cover classification to confine our data analysis to natural temperate and boreal vegetation at high and mid-northern latitudes. The UMd classification has a spatial resolution of 1 km for the entire globe (Hansen et al., 2000). We applied majority sampling to the UMd land-cover classification to harmonize the differences in spatial resolutions between UMd classification and GIMMS LAI3g (Park et al., 2018).

2.1.2 | Climate reanalysis and carbon dioxide concentrations

We used data from the European Centre for Medium Range Weather Forecasts Reanalysis 5 (ERA5; Hersbach et al., 2020) to identify climatic variables that could influence RVG. ERA5 is a state-of-the-art reanalysis dataset providing various atmospheric and surface variables every hour on a 0.25 × 0.25° latitude–longitude grid, with an improved data assimilation system and model physics compared to its previous version, ERA-Interim (Hersbach et al., 2020). We used air temperature at 2 m, surface net solar radiation, and total precipitation to analyze the responses of RVG to environmental conditions. The ERA5 data were harmonized to the spatial resolution of the LAI dataset using nearest-neighbor interpolation to ensure consistency in analyses (Park et al., 2018).

To consider a possible effect of atmospheric carbon dioxide concentrations on the RVG, carbon dioxide concentrations measured at the Barrow Atmospheric Baseline Observatory (BRW) in Alaska (71.3°N,

156.6°W) by the National Oceanic and Atmospheric Administration Earth System Research Laboratory were used. The BRW has been measuring atmospheric carbon dioxide concentration since the early 1970s, and serves as a robust representative of a long-term carbon dioxide record. The data collected covers the northern high-latitude regions and has been used in numerous studies (Gonsamo et al., 2018; Jeong et al., 2018; Park et al., 2019; Piao et al., 2020).

2.2 | Method

2.2.1 | Calculation of RVG and phenological variables

We calculated RVG for deciduous vegetation between 30 and 80°N for 1982–2016. RVG is a large-scale measure of the speed of vegetation growth during the green-up stage from winter dormancy to summer maturity. We applied Savitzky–Golay filtering on the LAI time series, following Chen et al. (2004), to minimize the potential influence of snow or cloud contamination. Then, we calculated RVG based on an optimized logistic curve that fitted to the filtered LAI time series from January 1 to the date of maximum LAI of each year (Atkinson et al., 2012; Julien & Sobrino, 2009; Park et al., 2015; Zhang et al., 2003).

$$\mathrm{LAI}(t) = \frac{-c}{1+\exp(-a(1-bt))} + d.$$

LAI was formulized as a function of the day of year (t) with four coefficients (a, b, c, and d) obtained from the fitting. The start of the growing season (SOS) is defined as the date of inflection ($1/b$) in the logistic curve, that is, the date of maximum LAI increasing rate (Park et al., 2015; Zhang et al., 2003). This inflection date corresponds to the date when LAI reaches 50% of its annual amplitude as well (Gonsamo et al., 2018). RVG was defined as the maximum rate of increase in LAI at SOS normalized by the annual amplitude (c in the above equation). Normalization reduces the influence of changes in maximum LAI on RVG, which is an effect of an increase or decrease in biomass rather than of the acceleration of the speed of growth. RVG can be expressed as:

$$\mathrm{RVG} = \frac{1}{c}\left(\frac{\partial}{\partial t}\mathrm{LAI}\right)_{t=\frac{1}{b}} = \frac{ab}{4}.$$

The unit of RVG, d^{-1}, was converted to % mon^{-1} by multiplying by 100% and 30 days for convenience in the present study. If the RVG of a biome is 80% mon^{-1}, then the biome acquires approximately 80% of the seasonal amplitude in a month. Therefore, we focused on the relative rate of increase in LAI, which represents growth rather than the amount of biomass. The RVG was calculated for regions where the LAI amplitude was >1 m^2/m^2 to focus on robust deciduous vegetation.

We also calculated the date of pregreen-up (DPG) and the start of the peak growing season (SOP) to reveal the vegetation green-up dynamics in spring. DPG and SOP are defined as the dates when LAI reaches 20% and 80% of its annual amplitude, respectively, according to previous studies (Kern et al., 2020; Wang et al., 2018), indicating the timing of the earliest start and the peak of spring growth, respectively. DPG represents the early stage of spring growth that precedes the green-up date (i.e., SOS) and potentially influences the subsequent green-up processes, that is, RVG. Kern et al. (2020) reported that an advance in pregreen-up could lead to a longer duration of green-up in Central Europe, which would be observed as an increase in RVG. DPG and SOP were calculated based on the linearly interpolated daily LAI time series after Savitzky–Golay filtering (Chen et al., 2004) for each data pixel to indicate the start and peak of the green-up stage. We also tested different thresholds and interpolation methods; however, these did not result in a noticeable change in the major findings of this study. Logistic curve fitting was not used for determining DPG or SOP to avoid a possible statistical dependency with RVG.

2.2.2 | Selection of environmental variables and partial correlation analyses

Various environmental variables, such as temperature sum, chilling days, photocondition, and precipitation influence the green-up stage (Delpierre et al., 2016; Fu et al., 2015; Hänninen & Kramer, 2007; Kern et al., 2020; Piao et al., 2020). Here we defined four variables that could influence interannual and long-term variations in RVG, including growing degree-day (GD), solar radiation (RD), chilling exposure (CE), and accumulated precipitation (PR), based on an ERA5 reanalysis for each data point and year as follows:

$$\mathrm{GD} = \sum_{t=\mathrm{Jan\ 1st}}^{\mathrm{SOS_{clim}}} \begin{cases} 0 & \text{for } T(t) < 0°\mathrm{C} \\ T(t) - 0°\mathrm{C} & \text{for } T(t) \geq 0°\mathrm{C} \end{cases},$$

$$\mathrm{RD} = \sum_{t=\mathrm{SOS_{clim}}-15}^{\mathrm{SOS_{clim}}+15} R(t),$$

$$\mathrm{CE} = \sum_{t=\mathrm{Jan\ 1st}}^{\mathrm{SOS_{clim}}} \begin{cases} 0 & \text{for } T(t) < 0°\mathrm{C} \\ 1 & \text{for } 0°\mathrm{C} \leq T(t) \leq 5°\mathrm{C} \\ 0 & \text{for } T(t) > 5°\mathrm{C} \end{cases},$$

$$\mathrm{PR} = \sum_{t=\mathrm{Nov\ 1st}}^{\mathrm{SOS_{clim}}} P(t),$$

where $T(t)$, $R(t)$, and $P(t)$ denote daily temperature at 2 m, surface net solar radiation, and total precipitation, respectively, from the ERA5 reanalysis as a function of the day of year (t), and $\mathrm{SOS_{clim}}$ indicates climatological SOS averaged over the entire research period for each data-point.

The four climatic variables represent general environmental conditions of temperature, radiation, and precipitation during the early green-up stage before SOS. GD represents the accumulated temperature above the base temperature (i.e., 0°C) from the first day of a year, which accelerates the overall vegetation growth. GD is based on the concept of thermal time that has been used extensively (Delpierre et al., 2016). Although the optimal base temperature could differ according to tree species (Klosterman et al., 2018), the base temperature was set at 0°C, following Fu et al. (2016). The major findings of the study were not affected by the adjusted base temperature. RD measures the intensity of surface solar radiation absorbed for 31 day around SOS. Photoconditions can regulate the seasonal growth of vegetation at high latitudes (Bonan & Shugart, 1989), and high light intensity can accelerate green-up processes in some plant species (Caffarra & Donnelly, 2011; Kern et al., 2020). The time window for calculating RD was set to 31 day around the climatological SOS to minimize potential collinearity with GD using a different time window. CE is a measure of exposure to chilling, that is, the number of days when the daily temperature is >0 and <5°C. Such exposure could accelerate green-up by reducing heat requirements (Cannell & Smith, 1983; Delpierre et al., 2016; Fu et al., 2015; Seyednasrollah et al., 2018; Yu et al., 2010). PR represents the amount of precipitation accumulated from November 1st of the preceding year until the climatological SOS, which can have an ancillary influence on vegetation growth by modifying the balance of surface energy (Yun et al., 2018) or enhancing water availability (Kern et al., 2020; Seyednasrollah et al., 2018; Xu et al., 2016). We tested several sets of different thresholds and temporal windows for the climate variables; however, these did not result in noticeable changes in the major finding of this study.

Together with the four climatic variables above, two non-climatic independent variables, DPG and atmospheric carbon dioxide concentration, were included in the multivariable analyses. The late DPG can increase the rate of green-up (Kern et al., 2020; Klosterman et al., 2018); thus, we used DPG of each data point to understand the interannual and long-term changes in RVG. In addition, an increase in atmospheric carbon dioxide concentration could alter plant structures and the development of leaves (Pritchard et al., 1999). To consider this effect on a long-term basis, annual mean carbon dioxide concentrations recorded at BRW (hereafter CO_2) were also included in the variable set as a representative of high-latitude carbon dioxide concentration.

The set of six environmental variables were composed of the four climatic and two non-climatic predictors, that is, GD, RD, CE, PR, DPG, and CO_2, to conduct partial correlation analyses to examine the interannual relationships between RVG and the environmental conditions in study regions where RVG was observed for >20 years. Partial correlation analysis is a useful tool for evaluating relationships between dependent and independent variables by linearly controlling other independent variables (Park et al., 2018; Peng et al., 2013). For the partial correlation analyses, all variables were linearly detrended to focus on the interannual relationships by eliminating the effect of long-term change in each variable (Fu et al., 2015; Wang et al., 2018). We used the approach to examine the interannual relationships between RVG and the six variables in the northern extratropics over the 35 year study period (1982–2016).

2.2.3 | Multivariable linear regression

We used a multilinear regression analysis to estimate the influence of environmental conditions on the long-term RVG changes. The multilinear regression was formularized based on the six variables as follows:

$$\mathrm{RVG}(t) = a_{\mathrm{GD}}\mathrm{GD}(t) + a_{\mathrm{RD}}\mathrm{RD}(t) + a_{\mathrm{CE}}\mathrm{CE}(t) + a_{\mathrm{PR}}\mathrm{PR}(t) + a_{\mathrm{DPG}}\mathrm{DPG}(t) + a_{\mathrm{CO_2}}\mathrm{CO_2}(t) + \varepsilon(t) + b.$$

RVG was expressed by a linear combination of the six variables using the above equation with an error term, $\varepsilon(t)$. The regression coefficients (a_{GD}, a_{RD}, a_{CD}, a_{PR}, a_{DPG}, $a_{\mathrm{CO_2}}$, and b), indicate the sensitivities of RVG to each variable, and an intercept (b), were trained using a multilinear regression based on RVG and the time series of the six variables at each data point for the entire study period. The regressed $\mathrm{RVG_{reg}}$ based on the six variables could be formulized by disregarding the error term, as follows:

$$\mathrm{RVG_{reg}}(t) = a_{\mathrm{GD}}\mathrm{GD}(t) + a_{\mathrm{RD}}\mathrm{RD}(t) + a_{\mathrm{CE}}\mathrm{CE}(t) + a_{\mathrm{PR}}\mathrm{PR}(t) + a_{\mathrm{DPG}}\mathrm{DPG}(t) + a_{\mathrm{CO_2}}\mathrm{CO_2}(t) + b.$$

By obtaining a time derivative of the above equation, $\mathrm{RVG_{reg}}$ could be decomposed into the long-term trends of the contributions of each variable as follows:

$$\frac{d\mathrm{RVG_{reg}}}{dt} = a_{\mathrm{GD}}\frac{d\mathrm{GD}}{dt} + a_{\mathrm{RD}}\frac{d\mathrm{RD}}{dt} + a_{\mathrm{CE}}\frac{d\mathrm{CE}}{dt} + a_{\mathrm{PR}}\frac{d\mathrm{PR}}{dt} + a_{\mathrm{DPG}}\frac{d\mathrm{DPG}}{dt} + a_{\mathrm{CO_2}}\frac{d\mathrm{CO_2}}{dt}.$$

We used the equation to estimate the influence of each variable $\left(\text{i.e., } a_{\mathrm{GD}}\frac{d\mathrm{GD}}{dt},\ a_{\mathrm{RD}}\frac{d\mathrm{RD}}{dt},\ a_{\mathrm{CE}}\frac{d\mathrm{CE}}{dt},\ a_{\mathrm{PR}}\frac{d\mathrm{PR}}{dt},\ a_{\mathrm{DPG}}\frac{d\mathrm{DPG}}{dt},\ \text{and } a_{\mathrm{CO_2}}\frac{d\mathrm{CO_2}}{dt}\right)$ on the $\mathrm{RVG_{reg}}$ trend, which was a linearly approximated RVG based on the six variables selected, for the regions with ≥20 years of RVG data. It is a simple but accessible tool for determining the key variable influencing the long-term changes in the dependent variable (RVG) under an assumption of linearity (Park et al., 2018). We used the six environmental variables and linear decomposition to examine the long-term RVG trends and their causes in the regions in recent decades.

3 | RESULTS

3.1 | Relationship between RVG and peak of growing season

Figure 1 shows spatial patterns of RVG and SOP with their distributional and interannual relationships in the northern extratropics.

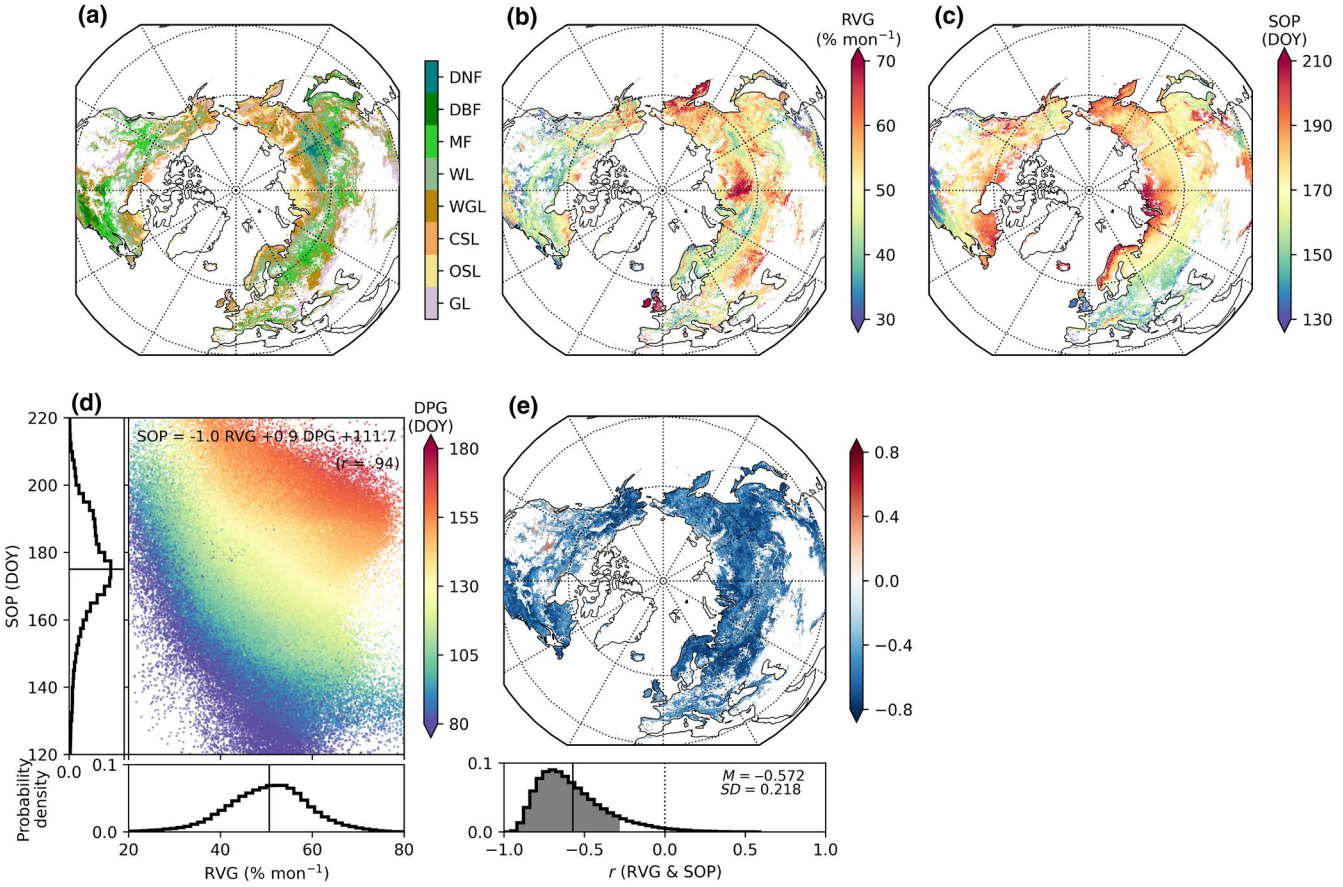

FIGURE 1 Spatial distribution of (a) eight deciduous vegetation types, (b) the rate of vegetation green-up (RVG), and (c) the start of the peak growing season (SOP) for the northern extratropics from 1982 to 2016. (d) Scatter plot of the climatological RVG, SOP, and the date of pregreen-up (DPG) with probability density functions. (e) Correlation map of RVG and SOP in the northern extratropics from 1982 to 2016. DNF, DBF, MF, WL, WGL, CSL, OSL, and GL indicate deciduous needleleaf forest, deciduous broadleaf forest, mixed forest, woodland, wooded grassland, closed shrubland, open shrubland, and grassland, respectively. The probability density function (shaded where $p < .1$) with its mean (M; marked by vertical line) and standard deviation (SD) are also denoted [Colour figure can be viewed at wileyonlinelibrary.com]

Figure 1a shows the distribution of eight deciduous vegetation types used in this study; deciduous needleleaf forest, deciduous broadleaf forest, mixed forest, woodland, wooded grassland, closed shrubland, open shrubland, and grassland, respectively. The regions with weak LAI amplitude (<1 m^2/m^2) were excluded to focus on deciduous vegetation with robust seasonality. Figure 1b presents the spatial distribution of RVG climatology in the region of interest during the entire study period. RVG ranged from approximately 30% to 70% mon^{-1} and tended to be higher at high-latitude regions such as Siberia, Kamchatka Peninsula, and Alaska. The high RVG indicates rapid development of the vegetation during green-up. This latitudinal dependence was more distinct in North America than in Eurasia. Along the same latitude, RVG was higher for vegetation in Eurasia than for vegetation in North America, indicating that vegetation tended to grow more rapidly in Eurasia.

Figure 1c presents the average SOP distribution over the study period. SOP occurred from 120 to 220 days of the year at higher latitudes, indicating that high-latitude vegetation reached the peak season later than the mid-latitude vegetation. In comparison to the latitudinal patterns observed in RVG dependence, SOP exhibited a clear latitudinal dependence and increased with increasing latitude. SOP was often earlier in European regions, the Mediterranean Basin, and southeastern North America than in eastern Asia and subarctic regions.

We examined the spatial relationships between the distribution of RVG and SOP, and DPG (Figure 1d). Climatologically, the regions with higher RVGs tend to show earlier SOPs under similar DPG conditions. The relationships among the three factors above can be expressed as SOP = −1.0 RVG + 0.9 DPG + 111.7, indicating that an increase in RVG of 1% mon^{-1} would advance SOP by 1 day. Approximately 90% of the spatial variation of SOP was explained by the speed of growth and the timing of pregreen-up ($r = .94$), demonstrating the role of RVG in SOP distribution.

Figure 1e illustrates the interannual correlation between RVG and SOP time series. RVG was significantly ($p < .1$) and negatively correlated with SOP, that is, a higher RVG led to an earlier SOP throughout the entire region of interest. Approximately 98% of the data points were negatively correlated with SOP, and 91% of the negative correlations were significant. Consequently, Figure 1d,e concurrently show that the climatological and interannual variations in RVG influenced SOP in the northern extratropics.

3.2 | Long-term RVG trends

We investigated the RVG trends to clarify the long-term changes in green-up over recent decades. Figure 2 illustrates the spatial trends and time series of the RVG trends in Eurasia and North America from 1982 to 2016. RVG tended to be positive in 59% of the entire study region, and 32% of the positive trends (19% of all regions) were significant ($p < .1$; Figure 2a). The average, 25th and 75th percentiles of the trends in RVG were 0.7%, −1.3%, and 2.5% mon^{-1} decade^{-1}, respectively, over the entire region, and approximately 13% of the data points indicated a highly increasing RVG trend exceeding 4% mon^{-1} decade^{-1}. The strong positive trends were distinct in the subarctic regions of North America and Eurasia. In contrast, the trends were significantly negative in only 10% of the region of interest. The negative trends were mainly in the temperate and boreal regions of Eurasia, such as eastern Asia, Fennoscandia, and Siberia, rather than in the subarctic.

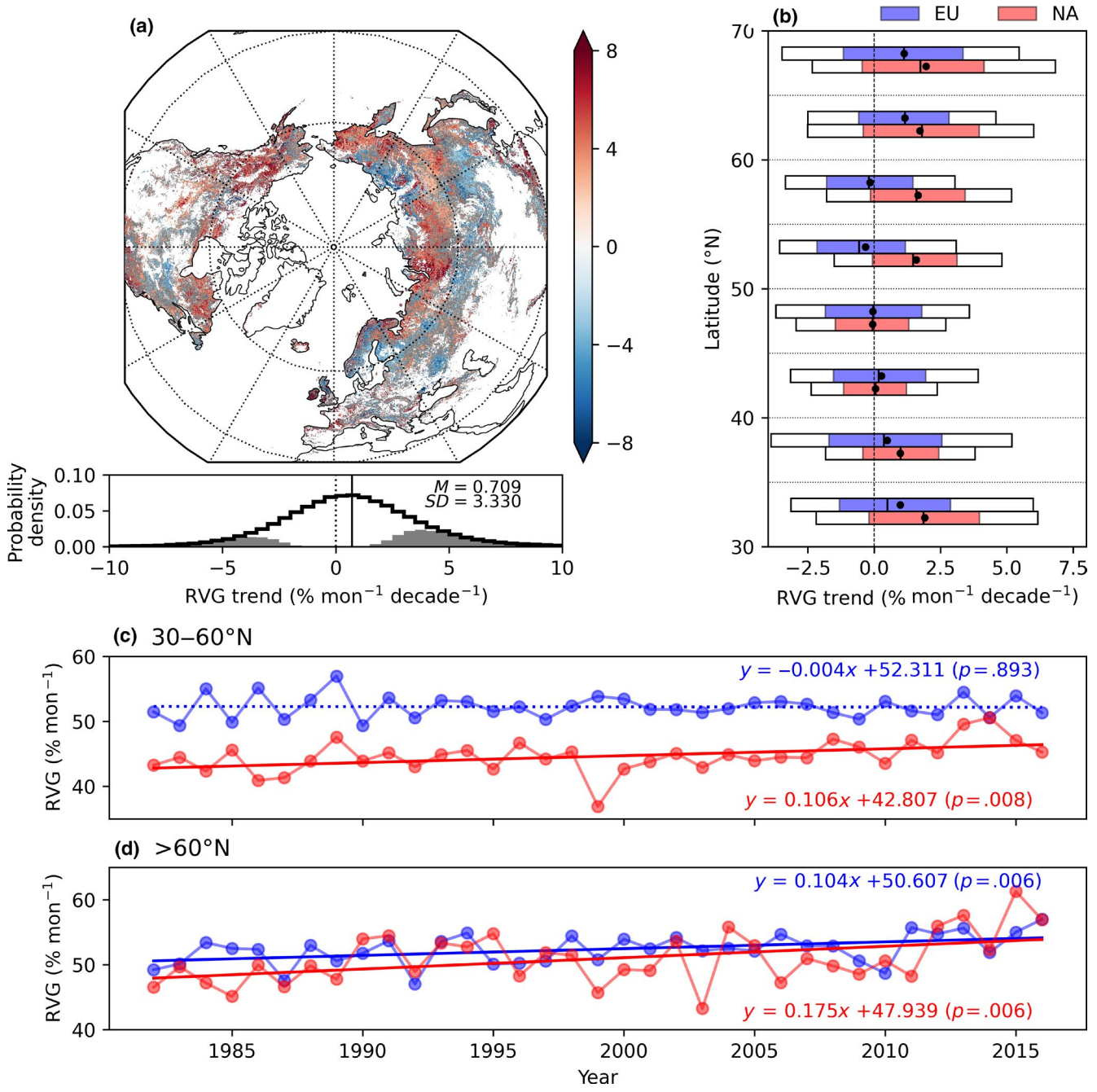

FIGURE 2 (a) Spatial distribution of RVG trends ($p < .1$ only) over the northern extratropics from 1982 to 2016 and its probability density function (shaded where $p < .1$) with mean (M; marked by vertical line) and standard deviation (SD). (b) Box plot of the RVG trends for each 5 degree latitude band from 30 to 75°N in Eurasia (EU, blue) and North America (NA, red). The ranges of 10th–90th (colored box), and 25th–75th percentiles (white box) are denoted with means (dot) and medians (vertical bar). (c) Time series of RVG and regression lines of Eurasia (blue) and North America (red) for the mid-latitude regions (30–60°N) from 1982 to 2016. (d) is same with (c) but for the high-latitude regions (>60°N) [Colour figure can be viewed at wileyonlinelibrary.com]

Figure 2b illustrates the RVG trends in 5° latitudinal bands for each continent. The zonal mean trends tended to increase from low- to high-latitude regions above the latitude of 40°N in both Eurasia and North America. Both Eurasian and North American vegetation showed strong positive RVG trends in the subarctic latitudes above 60°N. In Eurasia, the spatially averaged RVG trends were around zero from the latitude of 40–60°N, but in the subarctic regions, the majority of vegetation showed increasing RVG trends with time. Similarly, in North America, the RVG trends displayed greater values at higher latitudes (>50°N), and the positive RVG trends were stronger in North America when compared with Eurasia in most of the latitudinal bands. The zonal mean patterns showed that the strong and positive RVG trends were mainly distributed at latitudes higher than 60°N, indicating that high-latitude vegetation experienced considerable increases in RVG over time over the past three decades.

Figure 2c,d present RVG time-series at 30–60 and >60°N in Eurasia and North America. RVG was generally higher in Eurasia (52.3% mon^{-1} $decade^{-1}$) than in North America (44.6% mon^{-1} $decade^{-1}$) at the lower latitudes, although the temporal trends were relatively weak and not significant (−0.4% mon^{-1} $decade^{-1}$; $p > .1$; Figure 2c). RVG in North American vegetation tended to be significantly positive by 1.1% mon^{-1} $decade^{-1}$ ($p < .01$), and the difference in RVG between the continents decreased with time; from 8.6% mon^{-1} in 1982–2001 to 5.4% mon^{-1} in 2007–2016. Compared to the lower latitudes, the averages did not vary with continents as distinctly at high latitudes (Figure 2d). RVG for high-latitude vegetation was similar between Eurasia and North America, ranging from 40% to 60% mon^{-1}. Notably, RVG tended to increase in both Eurasia (1.0% mon^{-1} $decade^{-1}$) and North America (1.8% mon^{-1} $decade^{-1}$), with significant trends ($p < .01$) >60°N, as shown in the zonal mean pattern.

The RVG difference between continents decreased over the past decade (2007–2016), which can be attributed to the trends in North America being approximately twofold stronger than those in Eurasia. During 1982–1991, RVG was 49.1% and 51.4% mon^{-1} in North America and in Eurasia, respectively, but the difference of 2.3% mon^{-1} between the two continents decreased to only 0.3% mon^{-1} in the past decade. The results indicate that RVG significantly increased over high-latitude regions, particularly in North America, that is, velocity of green-up became faster in the recent decades. Therefore, we targeted the high-latitude regions (>60°N) to investigate the remarkable increases in RVG and the underlying mechanisms.

3.3 | Interannual relationships between RVG and the environmental variables

We examined the relationship of RVG with six environmental variables to determine the temporal changes in RVG over the high latitude regions. Figure 3 illustrates the partial correlations between RVG and the six variables focusing on strong RVG trends over the high latitudes above 60°N. The long-term trends in RVG and the independent variables are linearly detrended to focus on their interannual relationships. Figure 3a shows the partial correlation between RVG and GD, that is, the relationship between RVG and GD without the influence of other variables. RVG and GD were significantly positively correlated throughout all the study regions, indicating that high temperatures accelerated RVG, as previously reported (Park et al., 2015). Most of the data points were positive (76.8% of all the study regions), and the proportion of significantly negative data points was negligible (1.9%) when compared with the proportion of positive data points, indicating the positive influence of GD on RVG. Figure 3b shows the correlation between RVG and RD, revealing insolation during green-up. RD showed significantly positive correlations with RVG in most regions (approximately 29.1% of all data points), indicating strong increases in insolation during green-up, and the proportions of significantly negative correlations were negligible (1.7%). High temperatures and radiation were the key factors accelerating RVG at high latitudes (Figure 3a,b).

The patterns of partial correlation of RVG with CE and PR revealed auxiliary roles of chilling days and precipitation on green-up (Figure 3c,d). RVG and CE had a complex spatial pattern, with mixed positive and negative signals (Figure 3c), when compared to the widespread positive relationships illustrated in Figure 3a,b. RVG and CE were significantly positively correlated in 4.6% of the data points, indicating that cold temperatures ($0 < T < 5$°C) accelerated RVG; however, more data points were significantly negatively correlated (8.2%). The negative correlation indicated that cold temperature could hinder vegetation growth during green-up. Only 12.8% of the data points were significant, indicating that CE was not a major driver of the temporal changes in RVG at high latitudes. PR also exhibited mixed patterns of positive and negative correlations (Figure 3d), so that higher precipitation both increased and decreased RVG, similar to CE. RVG and PR were significantly positively and negatively correlated in 8.4% and 4.1% of the regions, respectively. CE and PR were correlated with RVG throughout the study regions, but the directions of the correlations differed with location, and the proportion of the significant correlations of CE and PR with RVG was minor compared to the correlations for GD and RD.

To explore the interannual influence of non-climatic variables on RVG, relationships among both DPG, CO_2, and RVG were examined. RVG and DPG were predominantly positively correlated, indicating that an earlier pregreen-up generally tended to decrease RVG (Figure 3e). Majority of the data points >60°N were positively correlated (84.0%), and 60.1% of the positive data points were significant. RVG and DPG were significantly negatively correlated in few regions, but only in 2.7% of the data points. The prevalence of significant positive correlation was consistent with the observations of Kern et al. (2020), who reported that earlier pregreen-up prolongs the duration from the pregreen-up to the mature state in Central Europe. Such green-up dynamics, that is, earlier start but slower growth, were predominant and significantly correlated with the RVG in high-latitude regions. Figure 3f shows that CO_2 had a complex pattern that comprised significant positive and negative correlations (8.8% and 6.8%), compared to the prevalent positive correlation of DPG. These minor correlations showed that the CO_2 did not exert a decisive influence on the interannual variation

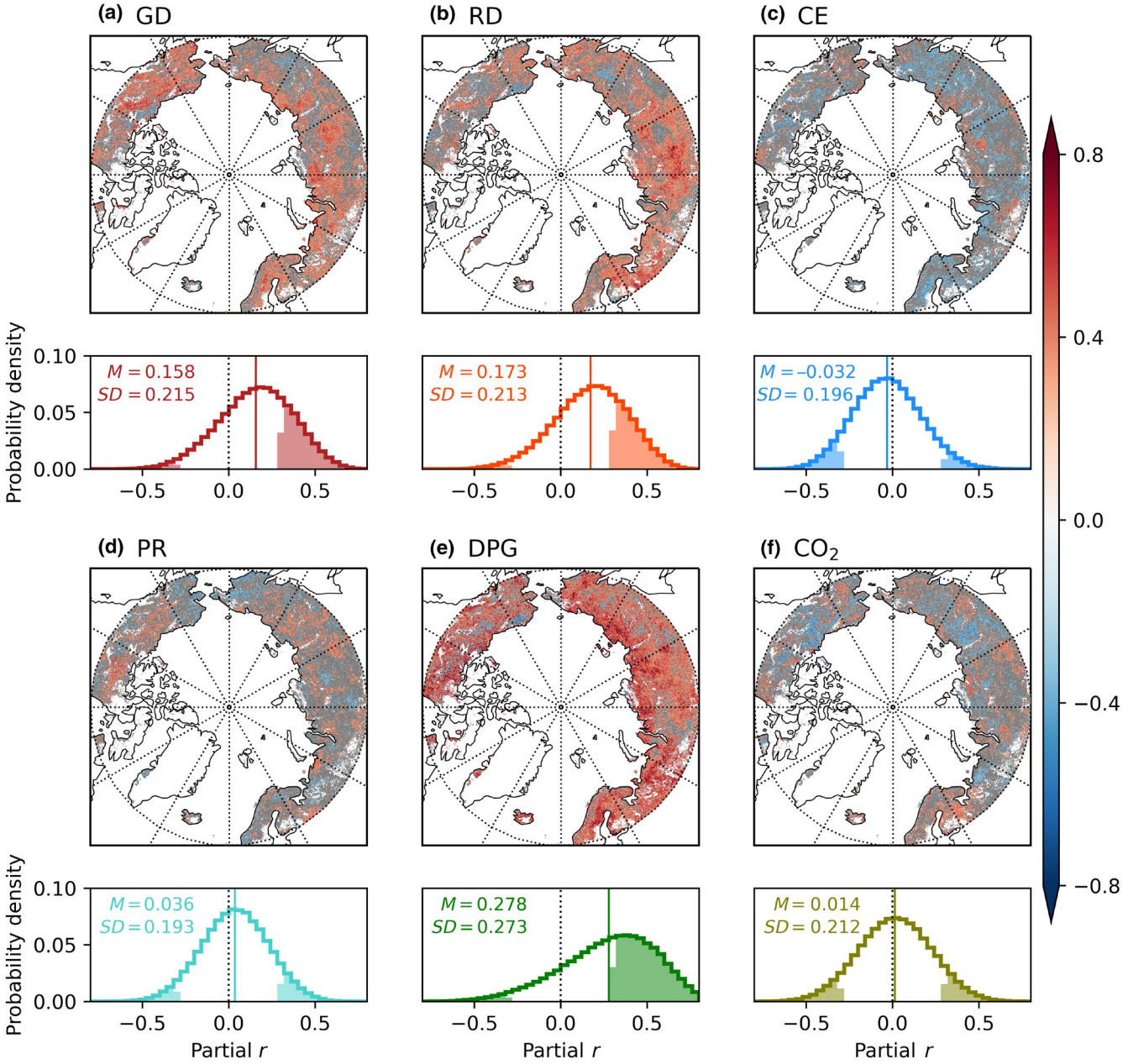

FIGURE 3 Spatial distributions of partial correlation coefficients between RVG and (a) GD, (b) RD, (c) CE, (d) PR, (e) DPG, and (f) CO_2 in the high latitudes ($p < .1$ only). Probability density functions (shaded where $p < .1$) of the partial correlations with mean (M; marked by vertical line) and standard deviation (SD) for each variable are also noted [Colour figure can be viewed at wileyonlinelibrary.com]

of RVG as similarly shown in CE and PR. Figure 3 indicates that GD, RD, and DPG were major factors closely related to the interannual variation in RVG at high latitudes, with ancillary influences of CE, PR, and CO_2.

3.4 | Acceleration and long-term drivers of RVG at high latitudes

We conducted multilinear regression analyses of the RVG trends using GD, RD, CE, PR, and PR to determine the influence of each variable on the long-term RVG trends based on an assumption of linearity. The correlation between RVG and RVG_{reg} indicated the reliability of the multilinear approach for the study of the interannual variation (Figure 4a). Approximately 70% of the data points showed high correlation coefficients ($r > .5$) at high latitudes, although the approach neglected nonlinear interactions of the RVG and the variables. Neither longitude nor latitude influenced the distribution, and the spatial mean of the correlation was 0.60, indicating that the multilinear regression could account for 36% of the interannual variations. The explanatory power was not ideal for comprehensively representing the interannual variation and was only because of a few anomalous peaks in the RVG time series, which will be discussed based on Figure 4c,d.

The spatial trends of RVG_{reg} were reconstructed using a multilinear approach (Figure 4b). The RVG_{reg} trend was similar to the RVG trend in Figure 1a. The RVG_{reg} trends were strongly positive in the subarctic regions of Eurasia and North America, similar to the RVG trends. The percentage of positive RVG_{reg} trends >60°N was 65.4%, and it was consistent with the RVG trend in Figure 2a, which was 65.3%. The RVG_{reg} trend also resembled the negative patterns in Fennoscandia and along the 60°N latitude (Figure 1a). The mean, 25th, and 75th percentiles were 1.2%, −0.9%, and 3.2% mon^{-1} $decade^{-1}$, respectively, which were same with those for RVG at one decimal place. Statistical measures were examined (e.g., the difference between RVG_{reg} trends and RVG trend, and variance inflation factors of each variable) to inspect the statistical validity, leading to a reasonable level of statistical robustness of the multilinear approach (Figures S1 and S2). These

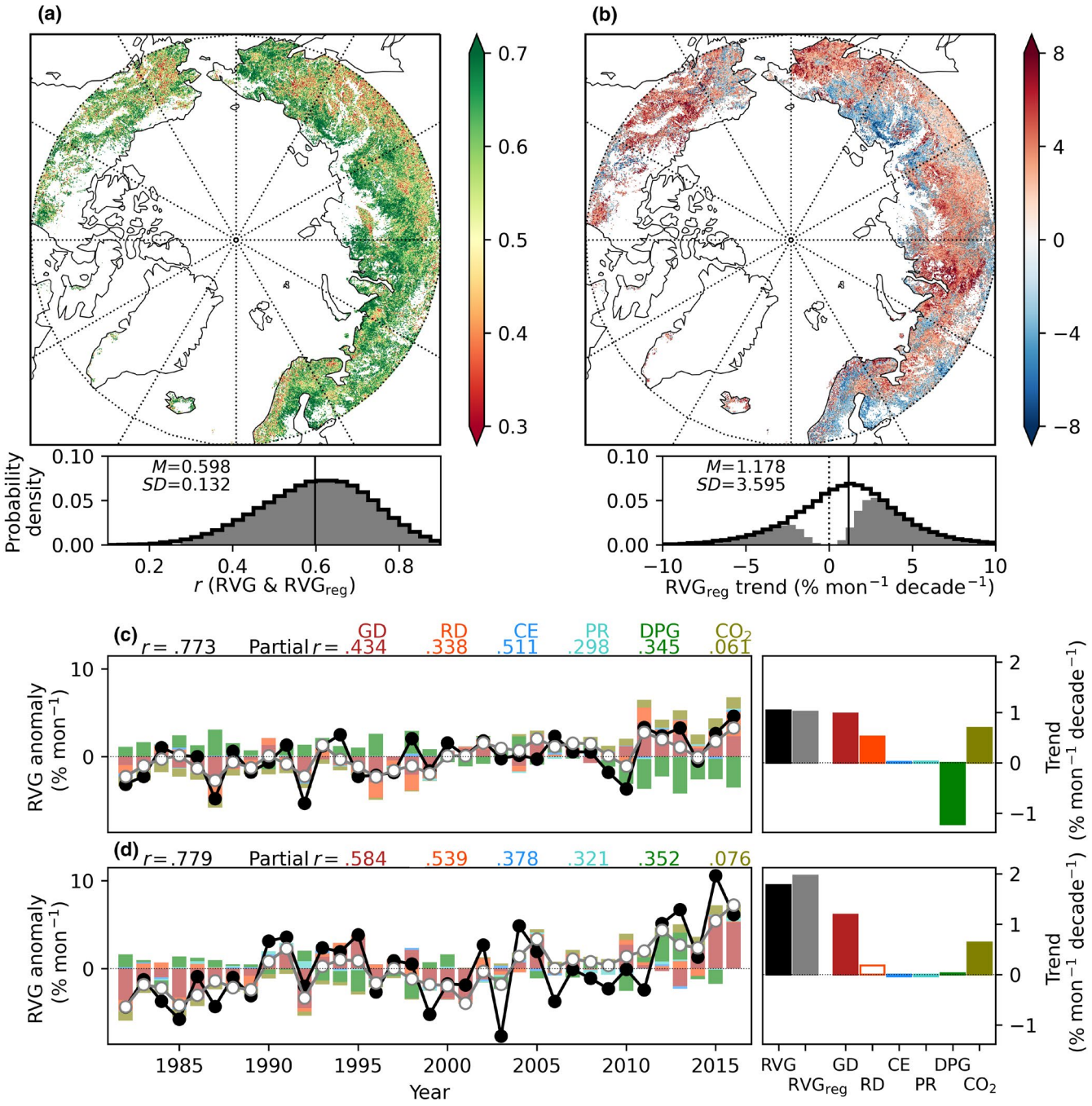

FIGURE 4 (a) Correlations between RVG and regressed RVG (RVG_{reg}), and (b) RVG_{reg} trends based on the multilinear regression of GD, RD, CE, PR, DPG, and CO2 in 1982–2016 ($p < .1$ only). Probability density functions (shaded where $p < .1$) with mean (*M*, marked by vertical line) and standard deviation (*SD*) are also noted. (c) Time series of RVG (black) and RVG_{reg} (gray), with influences (bars) of GD (red), RD (orange), CE (light blue), PR (cyan), DPG (green), and CO_2 (khaki) in Eurasia from 1982 to 2016 (d) is same with (c) but in North America. Correlations between RVG and RVG_{reg} and partial correlations of RVG with each variable are also noted. The bars in the graphs to the right indicate the RVG and RVG_{reg} trends and the influence of each variable (filled for $p < .1$) [Colour figure can be viewed at wileyonlinelibrary.com]

results showed that the multilinear approach could appropriately represent the major features of long-term trends in RVG in the high latitudes.

Figure 4c,d illustrate the time series of RVG, RVG_{reg}, and the contribution of each variable regionally averaged for Eurasia and North America. The RVG and RVG_{reg} time series were consistent interannually for both Eurasia ($r = .77$) and North America ($r = .78$), indicating that RVG_{reg} accounted for about a half of the interannual variations. The details, however, differed between Eurasia and North America. The RVG_{reg} trend was 1.0% mon^{-1} $decade^{-1}$ for Eurasia (Figure 4c), which accounts for 97% of the RVG trends. The RVG_{reg} trend was decomposed into the influence of each variable, with GD, RD, DPG, and CO_2 having considerable influence, 1.0%, 0.5%, −1.2%, and 0.7% mon^{-1} $decade^{-1}$, respectively. GD, therefore, was the primary driver of the increasing RVG trends, with RD and CO_2 having a supportive role (RVG increased because of increases in temperature, radiation, and CO_2 concentration), but was partly counteracted by the DPG trends (RVG decreased because of an earlier pregreen-up). The partial correlations between the regional means of the time series of RVG and the variables were strong for CE, GD, DPG, RD, PR, and CO_2 ($r = .51$, .43, .35, .34, .30, and .06, respectively). CE and RD, however, did not strongly influence the long-term trends, despite their interannual correlation. In contrast, CO_2 played a meaningful role on the long-term changes in RVG_{reg}, but not interannually.

The RVG and RVG_{reg} trends in North America were 1.8% and 2.0% mon^{-1} $decade^{-1}$, respectively. The RVG_{reg} trends were slightly overestimated by approximately 10% of the RVG trends, but the correlation coefficient between RVG and RVG_{reg} was similar ($r = .78$) with in Eurasia. The RVG_{reg} trend was primarily owing to the influence of the GD trend (1.2% mon^{-1} $decade^{-1}$), that is, RVG increased because of spring warming, with minor influences of the CO_2 and RD trends, 0.6% and 0.2% mon^{-1} $decade^{-1}$, respectively. The correlations between RVG and the variables were high for GD, RD, CE, DPG, PR, and CO_2 (coefficients of 0.58, 0.54, 0.38, 0.35, 0.32, and 0.08, respectively) in North America. The drivers of the increasing RVG trends differed between Eurasia, driven by GD, RD, and CO_2 but offset by DPG, and North America, affected by GD and CO_2 (Figure 4c).

4 | DISCUSSION

The present study investigated the long-term RVG trends and their dynamics based on a satellite-retrieved LAI dataset focusing on high northern latitudes. RVG has received little attention (Kern et al., 2020; Park et al., 2015; Wang et al., 2018) although it is a dynamic factor that can advance (or delays) vegetation maturity (Figure 1). RVG increased significantly with time, particularly at high latitudes (Figure 2), and varied according to environmental conditions (Figure 3). The long-term RVG trend in high-latitude regions was primarily attributed to warming in both Eurasia and North America (Figure 4).

Our findings implied that elevated temperatures led to more rapid growth and earlier maturity, which is consistent with the advancement of the start of peak growing season that has been reported in previous studies (Buitenwerf et al., 2015; Gonsamo et al., 2018; Wang & Wu, 2019; Xu et al., 2016). The results also suggest the earlier peak growing season toward spring was facilitated by the more rapid green-up. Warming at high latitudes is expected to continue and to worsen each decade because of climate change (Stocker et al., 2013). Therefore, the RVG is highly likely to increase with spring warming in future climate scenarios unless the RVG becomes saturated at a certain level. Furthermore, the more rapid RVG and earlier SOP will likely reinforce the feedbacks of energy, water, and carbon cycles between vegetation and climate (Gonsamo et al., 2018; Park et al., 2019; Penuelas et al., 2009; Piao et al., 2020).

Notably, Eurasian vegetation exhibited a different mechanism of accelerating RVG (Figure 4c), which is distinct from North America (Figure 4d). Warming was the common and primary factor influencing the RVG trends in the high-latitude regions; however, in Eurasia, the advance of DPG offset the influence of elevated temperature, increased radiation, and rising CO_2 concentrations on RVG (Figure 4c), suggesting that Eurasian vegetation has shifted its seasonal cycle toward earlier pregreen-up with slower green-up which restrains the RVG trends. Kern et al. (2020) reported that earlier pregreen-up prolongs the duration of the green-up stage in Central Europe, that is, slower RVG because of earlier DPG in the present study. Such green-up dynamics between RVG and DPG were also widespread at the high latitudes (Figure 3c) but the advance of DPG occurred only in Eurasia and played a key role by alleviating the major RVG trends that were induced by both increased temperature, insolation, and CO_2 concentrations. Consequently, vegetation in Eurasia and North America could exhibit different trends in green-up rates in future if the advancing pregreen-up trends persist only in Eurasia, for example, earlier pregreen-up but less accelerated green-up in Eurasia and more accelerated green-up in North America. In addition, future shifts in temperature and insolation patterns could alter the rate of green-up significantly considering the strong relationship with climate variables (Figure 3a,b). However, the green-up dynamics remain unclear, and should be investigated further to obtain insights on green-up stages and RVG shifts under future climate scenarios.

An increase in RVG, that is, the acceleration of green-up, could be the result of a three-way ecological change. Foliar ontogeny could be accelerated because of environmental changes. High temperatures can influence the entire trajectory of foliar development in the form of more leaves or more rapid expansion (Way & Oren, 2010). Elevated CO_2 concentrations also can alter canopy architecture, increasing branching and leaf number per plant (Pritchard et al., 1999). Changes in environmental conditions in the subarctic regions could influence such fundamental processes of foliar and canopy development, and can be manifested as the increasing RVG trends based on satellite vegetation indices (Park et al., 2015). In addition, rapid green-up could be a

product of the synchronization of foliar unfolding among coexisting species (Mulder & Spellman, 2019). Leaves in a biome tend to unfold earlier in the understory than in the overstory species to maximize growth and survival (Richardson & O'Keefe, 2009; Ryu et al., 2014). If the difference in unfolding date between species decreases because of a change in environmental conditions, RVG could be accelerated by the synchronization of foliar emergence among species without any changes in foliar developmental processes. Furthermore, natural or anthropogenic changes in species composition due to climate change could cause long-term shifts in RVG trends. Changes in species composition due to succession or migration cannot account for the interannual variation in RVG because they occur over extended time scales; however, change in species could partly influence the long-term RVG trends in Eurasia and North America. Nevertheless, in situ observations or surface digital camera imagery would be required to determine the underlying phenomena driving RVG based on satellite-retrieved data despite the merits of satellite-based approaches that use long-term records over large spatial scales.

The present study was limited by the lack of consideration of nonlinear features of RVG in the multilinear approach. The multilinear regression was utilized to create an illustration of the influence of environmental variables on the long-term RVG trends, rather the interannual variations. The method was simple but effectively demonstrated the long-term behavior of the green-up stage and its major drivers (Figure 4). However, it was not ideal to explain the interannual variations in RVG, particularly in North America (Figure 4d), which seem to be contributed by the nonlinearity of RVG. Park et al. (2015) reported that RVG responded nonlinearly and strongly to an increase in temperature, that is, RVG responded more strongly to positive temperature anomalies than to negative temperature anomalies. Notably, RVG_{reg} could not fully account for the irregular peaks in RVG of the year of 2003 and 2015 (Figure 4d). Such gaps in the RVG peaks were responsible for the weak correlation between RVG and RVG_{reg} for North America (Figure 4a). The peaks could have been because of nonlinear characteristics of RVG that cannot be accounted for by assumptions of linearity. Chilling requirements could also influence RVG. Chilling requirement fulfillment influences foliar emergence by regulating heat requirements (Cannell & Smith, 1983; Fu et al., 2015) and can nonlinearly influence RVG. CE was included in the multilinear regression, but such a reciprocal effect between the variables, for example, a potential change in RVG sensitivity to GD (a_{GD}) when CE is high, could not be described appropriately under the assumption of linearity. This study cannot fully describe the interannual variation of RVG due to the limitation of the linear approach; however, the nonlinearity in RVG needs to be clarified for better understanding of the complicated behavior of the green-up stage in future studies.

The linear approach partitioned the long-term RVG trends into contributions of each of the six environmental variables; however, it is not an ideal and errorless tool to interpret the long-term RVG changes. The linear regression could misinterpret an unrelated but common trend in dependent and independent variables as a causal relationship between them. For example, CO_2 was almost monotonically increased for several decades, and played a secondary role on the long-term RVG trends. Physically, CO_2 is an important factor affecting foliar development (Pritchard et al., 1999), which could have a remarkable influence on the RVG trends. However, owing to the monotonic increase, this statistical approach could have assessed the long-term CO_2 influence as a sum of not only the influence of actual CO_2 but also other variables, which were not included in the independent variable set. Therefore, this study could overestimate the influence of CO_2 on the RVG trends. Previously, Wang et al. (2018) suggested that human land management played an important role on the acceleration of green-up velocity on a global scale. In the present study, we focus on high-latitude regions where human-managed ecosystems are minor, but this anthropogenic influence or other environmental factors could exert an effect on the long-term RVG trends. Consequently, these aspects should be considered in future studies to enhance the understanding of the responses of green-up to climatic and non-climatic conditions.

The present study showed that seasonal increases in LAI have become more rapid owing to spring warming, particularly in the subarctic regions. Changes in the green-up stage could lead to discrepancies among satellite-based methods for retrieving phenological data that apply different criteria and thresholds, as discussed by Buitenwerf et al. (2015). If a biome has similar onset but a more rapid green-up because of spring warming, SOS could be estimated differently depending the thresholds of vegetation indices, whether focusing on the early or late stages of green-up (Buitenwerf et al., 2015; White et al., 2009). The increasing RVG trends could amplify the inconsistencies among satellite-based phenologies. Therefore, taking into account the entire green-up cycles is necessary to adequately track changes in vegetation seasonality in a warming world.

ACKNOWLEDGEMENTS

This work was supported by grants from the National Research Foundation (NRF) of Korea (MSIT; no. 2019R1C1C1004826 and 2019R1A2C3002868), Creative-Pioneering Researchers Program of Seoul National University, and the European Research Council Synergy (no. ERC-2013-SyG-610028 IMBALANCE-P).

DATA AVAILABILITY STATEMENT

The GIMMS LAI3g dataset are available on request from Zaichun Zhu (zhu.zaichun@pku.edu.cn). The ERA5 is available in Copernicus Climate Change Service Climate Data Store (https://cds.climate.copernicus.eu/). The UMd global land cover classification was officially distributed by Global Land Cover Facility from University of Maryland, but shut down from the early of 2019. The UMd land-cover classification is currently available in IRI/LDEO Climate Data Library (https://iridl.ldeo.columbia.edu).

ORCID

Hoonyoung Park https://orcid.org/0000-0002-7856-5218
Sujong Jeong https://orcid.org/0000-0003-4586-4534
Josep Peñuelas https://orcid.org/0000-0002-7215-0150

REFERENCES

Atkinson, P. M., Jeganathan, C., Dash, J., & Atzberger, C. (2012). Inter-comparison of four models for smoothing satellite sensor time-series data to estimate vegetation phenology. *Remote Sensing of Environment*, *123*, 400–417. https://doi.org/10.1016/j.rse.2012.04.001

Badeck, F. W., Bondeau, A., Bottcher, K., Doktor, D., Lucht, W., Schaber, J., & Sitch, S. (2004). Responses of spring phenology to climate change. *New Phytologist*, *162*(2), 295–309.

Baldocchi, D. D. (2020). How eddy covariance flux measurements have contributed to our understanding of Global Change Biology. *Global Change Biology*. https://doi.org/10.1111/gcb.14807

Bonan, G. B., & Shugart, H. H. (1989). Environmental factors and ecological processes in boreal forests. *Annual Review of Ecology and Systematics*, *20*(1), 1–28. https://doi.org/10.1146/annurev.es.20.110189.000245

Buitenwerf, R., Rose, L., & Higgins, S. I. (2015). Three decades of multi-dimensional change in global leaf phenology. *Nature Climate Change*, *5*(4), 364–368. https://doi.org/10.1038/nclimate2533

Caffarra, A., & Donnelly, A. (2011). The ecological significance of phenology in four different tree species: Effects of light and temperature on bud burst. *International Journal of Biometeorology*, *55*(5), 711–721. https://doi.org/10.1007/s00484-010-0386-1

Cannell, M. G. R., & Smith, R. I. (1983). Thermal time, chill days and prediction of budburst in *Picea sitchensis*. *The Journal of Applied Ecology*, *20*(3), 951. https://doi.org/10.2307/2403139

Chen, J., Jönsson, P., Tamura, M., Gu, Z., Matsushita, B., & Eklundh, L. (2004). A simple method for reconstructing a high-quality NDVI time-series data set based on the Savitzky–Golay filter. *Remote Sensing of Environment*, *91*(3–4), 332–344. https://doi.org/10.1016/j.rse.2004.03.014

Clark, J. S., Salk, C., Melillo, J., & Mohan, J. (2014). Tree phenology responses to winter chilling, spring warming, at north and south range limits. *Functional Ecology*, *28*(6), 1344–1355. https://doi.org/10.1111/1365-2435.12309

Delpierre, N., Vitasse, Y., Chuine, I., Guillemot, J., Bazot, S., Rutishauser, T., & Rathgeber, C. B. K. (2016). Temperate and boreal forest tree phenology: From organ-scale processes to terrestrial ecosystem models. *Annals of Forest Science*, *73*(1), 5–25. https://doi.org/10.1007/s13595-015-0477-6

Fu, Y. H., Liu, Y., De Boeck, H. J., Menzel, A., Nijs, I., Peaucelle, M., & Janssens, I. A. (2016). Three times greater weight of daytime than of night-time temperature on leaf unfolding phenology in temperate trees. *New Phytologist*, *212*(3), 590–597. https://doi.org/10.1111/nph.14073

Fu, Y. H., Zhao, H., Piao, S., Peaucelle, M., Peng, S., Zhou, G., & Janssens, I. A. (2015). Declining global warming effects on the phenology of spring leaf unfolding. *Nature*, *526*(7571), 104–107. https://doi.org/10.1038/nature15402

Gonsamo, A., Chen, J. M., & Ooi, Y. W. (2018). Peak season plant activity shift towards spring is reflected by increasing carbon uptake by extratropical ecosystems. *Global Change Biology*, *24*(5), 2117–2128. https://doi.org/10.1111/gcb.14001

Hänninen, H., & Kramer, K. (2007). A framework for modelling the annual cycle of trees in boreal and temperate regions. *Silva Fennica*, *41*(1). https://doi.org/10.14214/sf.313

Hansen, M. C., Sohlberg, R., Defries, R. S., & Townshend, J. R. G. (2000). Global land cover classification at 1 km spatial resolution using a classification tree approach. *International Journal of Remote Sensing*, *21*(6–7), 1331–1364. https://doi.org/10.1080/014311600210209

Hersbach, H., Bell, B., Berrisford, P., Hirahara, S., Horányi, A., Muñoz-Sabater, J., … Simmons, A. (2020). The ERA5 global reanalysis. *Quarterly Journal of the Royal Meteorological Society*, *146*(730), 1999–2049.

Jeong, S. J., Bloom, A. A., Schimel, D., Sweeney, C., Parazoo, N. C., Medvigy, D., & Miller, C. E. (2018). Accelerating rates of Arctic carbon cycling revealed by long-term atmospheric CO_2 measurements. *Science Advances*, *4*(7), eaao1167. https://doi.org/10.1126/sciadv.aao1167

Jeong, S. J., Ho, C. H., Gim, H. J., & Brown, M. E. (2011). Phenology shifts at start vs. end of growing season in temperate vegetation over the Northern Hemisphere for the period 1982–2008. *Global Change Biology*, *17*(7), 2385–2399. https://doi.org/10.1111/j.1365-2486.2011.02397.x

Julien, Y., & Sobrino, J. A. (2009). Global land surface phenology trends from GIMMS database. *International Journal of Remote Sensing*, *30*(13), 3495–3513. https://doi.org/10.1080/01431160802562255

Kern, A., Marjanović, H., & Barcza, Z. (2020). Spring vegetation green-up dynamics in Central Europe based on 20-year long MODIS NDVI data. *Agricultural and Forest Meteorology*, *287*, 107969. https://doi.org/10.1016/j.agrformet.2020.107969

Klosterman, S., Hufkens, K., & Richardson, A. D. (2018). Later springs green-up faster: The relation between onset and completion of green-up in deciduous forests of North America. *International Journal of Biometeorology*, *62*(9), 1645–1655.

Menzel, A., Sparks, T. H., Estrella, N., Koch, E., Aasa, A., Ahas, R., & Zust, A. (2006). European phenological response to climate change matches the warming pattern. *Global Change Biology*, *12*(10), 1969–1976. https://doi.org/10.1111/j.1365-2486.2006.01193.x

Mulder, C. P. H., & Spellman, K. V. (2019). Do longer growing seasons give introduced plants an advantage over native plants in interior Alaska? *Botany-Botanique*, *97*(6), 347–362. https://doi.org/10.1139/cjb-2018-0209

Park, H., Jeong, S. J., Ho, C. H., Kim, J., Brown, M. E., & Schaepman, M. E. (2015). Nonlinear response of vegetation green-up to local temperature variations in temperate and boreal forests in the Northern Hemisphere. *Remote Sensing of Environment*, *165*, 100–108. https://doi.org/10.1016/j.rse.2015.04.030

Park, H., Jeong, S. J., Ho, C. H., Park, C. E., & Kim, J. (2018). Slowdown of spring green-up advancements in boreal forests. *Remote Sensing of Environment*, *217*, 191–202. https://doi.org/10.1016/j.rse.2018.08.012

Park, T., Chen, C., Macias-Fauria, M., Tømmervik, H., Choi, S., Winkler, A., & Myneni, R. B. (2019). Changes in timing of seasonal peak photosynthetic activity in northern ecosystems. *Global Change Biology*, *25*(7), 2382–2395. https://doi.org/10.1111/gcb.14638

Peng, S., Piao, S., Ciais, P., Myneni, R. B., Chen, A., Chevallier, F., & Zeng, H. (2013). Asymmetric effects of daytime and night-time warming on Northern Hemisphere vegetation. *Nature*, *501*(7465), 88–92. https://doi.org/10.1038/nature12434

Peñuelas, J., & Filella, I. (2001). Phenology: Responses to a warming world. *Science*, *294*(5543), 793–795. https://doi.org/10.1126/science.1066860

Penuelas, J., Rutishauser, T., & Filella, I. (2009). Phenology feedbacks on climate change. *Science*, *324*(5929), 887–888. https://doi.org/10.1126/science.1173004

Pettorelli, N., Vik, J. O., Mysterud, A., Gaillard, J. M., Tucker, C. J., & Stenseth, N. C. (2005). Using the satellite-derived NDVI to assess ecological responses to environmental change. *Trends in Ecology & Evolution*, *20*(9), 503–510. https://doi.org/10.1016/j.tree.2005.05.011

Piao, S., Wang, X., Park, T., Chen, C., Lian, X. U., He, Y., & Myneni, R. B. (2020). Characteristics, drivers and feedbacks of global greening. *Nature Reviews Earth & Environment*, *1*(1), 14–27. https://doi.org/10.1038/s43017-019-0001-x

Pritchard, S. G., Rogers, H. H., Prior, S. A., & Peterson, C. M. (1999). Elevated CO_2 and plant structure: A review. *Global Change Biology*, *5*(7), 807–837. https://doi.org/10.1046/j.1365-2486.1999.00268.x

Reed, B. C., Brown, J. F., VanderZee, D., Loveland, T. R., Merchant, J. W., & Ohlen, D. O. (1994). Measuring phenological variability from satellite imagery. *Journal of Vegetation Science*, *5*(5), 703–714. https://doi.org/10.2307/3235884

Richardson, A. D., Andy Black, T., Ciais, P., Delbart, N., Friedl, M. A., Gobron, N., & Varlagin, A. (2010). Influence of spring and autumn phenological transitions on forest ecosystem productivity. *Philosophical Transactions of the Royal Society B: Biological Sciences*, *365*(1555), 3227–3246. https://doi.org/10.1098/rstb.2010.0102

Richardson, A. D., Keenan, T. F., Migliavacca, M., Ryu, Y., Sonnentag, O., & Toomey, M. (2013). Climate change, phenology, and phenological control of vegetation feedbacks to the climate system. *Agricultural and Forest Meteorology*, *169*, 156–173. https://doi.org/10.1016/j.agrformet.2012.09.012

Richardson, A. D., & O'Keefe, J. (2009). Phenological differences between understory and overstory a case study using the long-term Harvard Forest records. In *Phenology of ecosystem processes: Applications in global change research* (pp. 87–117). New York, NYSpringer. https://doi.org/10.1007/978-1-4419-0026-5_4

Ryu, Y., Lee, G., Jeon, S., Song, Y., & Kimm, H. (2014). Monitoring multi-layer canopy spring phenology of temperate deciduous and evergreen forests using low-cost spectral sensors. *Remote Sensing of Environment*, *149*, 227–238. https://doi.org/10.1016/j.rse.2014.04.015

Schwartz, M. D. (2013). *Phenology: An integrative environmental science*. https://doi.org/10.1007/978-94-007-6925-0

Seyednasrollah, B., Swenson, J. J., Domec, J. C., & Clark, J. S. (2018). Leaf phenology paradox: Why warming matters most where it is already warm. *Remote Sensing of Environment*, *209*, 446–455. https://doi.org/10.1016/j.rse.2018.02.059

Stocker, T. F., Qin, D., Plattner, G. K., Tignor, M. M. B., Allen, S. K., Boschung, J., & Midgley, P. M. (2013). *Climate change 2013: The physical science basis*. Contribution of working group I to the fifth assessment report of the Intergovernmental Panel on Climate Change. Cambridge, UK: Cambridge University Press. https://doi.org/10.1017/CBO9781107415324

Wang, L., Tian, F., Wang, Y., Wu, Z., Schurgers, G., & Fensholt, R. (2018). Acceleration of global vegetation greenup from combined effects of climate change and human land management. *Global Change Biology*, *24*(11), 5484–5499. https://doi.org/10.1111/gcb.14369

Wang, X., & Wu, C. (2019). Estimating the peak of growing season (POS) of China's terrestrial ecosystems. *Agricultural and Forest Meteorology*, *278*, 107639. https://doi.org/10.1016/j.agrformet.2019.107639

Way, D. A., & Oren, R. (2010). Differential responses to changes in growth temperature between trees from different functional groups and biomes: A review and synthesis of data. *Tree Physiology*, *30*(6), 669–688. https://doi.org/10.1093/treephys/tpq015

White, M. A., de Beurs, K. M., Didan, K., Inouye, D. W., Richardson, A. D., Jensen, O. P., & Lauenroth, W. K. (2009). Intercomparison, interpretation, and assessment of spring phenology in North America estimated from remote sensing for 1982–2006. *Global Change Biology*, *15*(10), 2335–2359. https://doi.org/10.1111/j.1365-2486.2009.01910.x

Xu, C., Liu, H., Williams, A. P., Yin, Y., & Wu, X. (2016). Trends toward an earlier peak of the growing season in Northern Hemisphere mid-latitudes. *Global Change Biology*, *22*(8), 2852–2860. https://doi.org/10.1111/gcb.13224

Yu, H., Luedeling, E., & Xu, J. (2010). Winter and spring warming result in delayed spring phenology on the Tibetan Plateau. *Proceedings of the National Academy of Sciences of the United States of America*, *107*(51), 22151–22156. https://doi.org/10.1073/pnas.1012490107

Yun, J., Jeong, S. J., Ho, C. H., Park, C. E., Park, H., & Kim, J. (2018). Influence of winter precipitation on spring phenology in boreal forests. *Global Change Biology*, *24*(11), 5176–5187. https://doi.org/10.1111/gcb.14414

Zhang, X., Friedl, M. A., Schaaf, C. B., Strahler, A. H., Hodges, J. C. F., Gao, F., & Huete, A. (2003). Monitoring vegetation phenology using MODIS. *Remote Sensing of Environment*, *84*(3), 471–475. https://doi.org/10.1016/S0034-4257(02)00135-9

Zhu, Z., Bi, J., Pan, Y., Ganguly, S., Anav, A., Xu, L., & Myneni, R. B. (2013). Global data sets of vegetation leaf area index (LAI)3g and fraction of photosynthetically active radiation (FPAR)3g derived from global inventory modeling and mapping studies (GIMMS) normalized difference vegetation index (NDVI3G) for the period 1981 to 2. *Remote Sensing*, *5*(2), 927–948. https://doi.org/10.3390/rs5020927

Zhu, Z., Piao, S., Myneni, R. B., Huang, M., Zeng, Z., Canadell, J. G., & Zeng, N. (2016). Greening of the Earth and its drivers. *Nature Climate Change*, *6*(8), 791–795. https://doi.org/10.1038/nclimate3004

SUPPORTING INFORMATION

Additional supporting information may be found online in the Supporting Information section.

How to cite this article: Park H, Jeong S, Peñuelas J. Accelerated rate of vegetation green-up related to warming at northern high latitudes. *Glob Change Biol*. 2020;26:6190–6202. https://doi.org/10.1111/gcb.15322